0026-895X/04/6601-33–44$20.00
MOLECULAR PHARMACOLOGY
Copyright © 2004 The American Society for Pharmacology and Experimental Therapeutics
Mol Pharmacol 66:33–44, 2004

Vol. 66, No. 1
2989/1156957
Printed in U.S.A.

Mechanisms of Arsenic-Induced Prolongation of Cardiac Repolarization

Eckhard Ficker, Yuri A. Kuryshev, Adrienne T. Dennis, Carlos Obejero-Paz, Lu Wang, Peter Hawryluk, Barbara A. Wible, and Arthur M. Brown

Rammelkamp Center for Education and Research, MetroHealth Campus, Case Western Reserve University, Cleveland, Ohio (E.F., Y.A.K., A.T.D., L.W., A.M.B.); Department of Physiology and Biophysics, Case Western Reserve University, Cleveland, Ohio (C.O.-P.); and ChanTest, Inc., Cleveland, Ohio (P.H., B.A.W.)

Received September 22, 2003; accepted March 11, 2004

This article is available online at http://molpharm.aspetjournals.org

ABSTRACT

Arsenic trioxide (As_2O_3) produces dramatic remissions in patients with relapsed or refractory acute promyelocytic leukemia. Its clinical use is burdened by QT prolongation, torsade de pointes, and sudden cardiac death. In the present study, we analyzed the molecular mechanisms leading to As_2O_3-induced abnormalities of cardiac electrophysiology. Using biochemical and electrophysiological methods, we show that long-term exposure to As_2O_3 increases cardiac calcium currents and reduces surface expression of the cardiac potassium channel human *ether-a-go-go*-related gene (*HERG*) at clinically relevant concentrations of 0.1 to 1.5 μM. In ventricular myocytes, As_2O_3 increases action potential duration measured at 30 and 90% of repolarization. As_2O_3 interferes with hERG trafficking by inhibition of hERG-chaperone complexes and increases calcium currents by a faster cellular process. We propose that an increase in cardiac calcium current and reduced trafficking of hERG channels to the cell surface cause QT prolongation and torsade de pointes in patients treated with As_2O_3. Our results suggest that calcium-channel antagonists will be useful in normalizing QT prolongation during As_2O_3 therapy. As_2O_3 is the first example of a drug that produces hERG liability by inhibition of ion-channel trafficking. Other drugs that interfere with proteins in the processing pathway of cardiac ion channels may be proarrhythmic for similar reasons.

Arsenic has been used by physicians for more than 2000 years to treat diverse diseases ranging from cancer to syphilis and tuberculosis (Zhu et al., 2002). It was abandoned as a therapeutic drug only in the last century because of its broad toxicity, which is responsible for its use and reputation as a poison. Arsenic is believed to cause widespread organ damage by combining with neighboring thiol groups present in many proteins, and exposure may result in severe long- or short-term illness (Miller et al., 2002). Despite its well known toxicity, arsenic was rediscovered recently by modern medicine and is now in use worldwide after arsenic trioxide (As_2O_3) was identified as the active ingredient of traditional Chinese medicines that produced dramatic remissions in patients with relapsed or refractory acute promyelocytic leukemia (APL) (Soignet et al., 2001; Zhang et al., 2001; Barbey et al., 2003).

The therapeutic use of As_2O_3 in the treatment of APL is burdened by its toxicity; multiple adverse effects, including QT prolongation, torsade de pointes tachycardias (TdP), and sudden cardiac death, have been reported (St. Petery et al., 1970; Ohnishi et al., 2000; Unnikrishnan et al., 2001; Westervelt et al., 2001; Zhang et al., 2001). Although the metabolic toxicity of As_2O_3 may be attributed to the exquisite sensitivity of accessible thiol groups in key enzymes or to enzymes such as pyruvate dehydrogenase, which uses the dithiol lipoic acid as a cofactor (Miller et al., 2002), it remains entirely unclear by what mechanisms As_2O_3 induces electrocardiogram abnormalities (Little et al., 1990; Ohnishi et al., 2000; Unnikrishnan et al., 2001; Westervelt et al., 2001; Chiang et al., 2002). More recently, hereditary QT prolongation [long QT syndrome (LQTS)] has been linked to mutations in cardiac ion channels, notably hERG and KvLQT1 (Keating and Sanguinetti, 2001). In addition, drug-induced, acquired LQTS is often caused by direct blockade of the cardiac potassium channel hERG by a wide variety of structurally diverse therapeutic compounds (Redfern et al., 2003).

This work was supported by National Institutes of Health grants HL36930, HL61642, and HL55404 (to A.M.B.).

ABBREVIATIONS: As_2O_3, arsenic trioxide; APL, acute promyelocytic leukemia; TdP, torsade de pointes tachycardia; LQTS, long QT syndrome; hERG, human *ether a-go-go*-related gene; ER, endoplasmic reticulum; HA, hemagglutinin; ROS, radical oxygen species; APD, action potential duration; HP, holding potential; AP, action potential; MP, membrane potential; HEK, human embryonic kidney; PAO, phenyl arsine oxide; WT, wild-type; I-V, current-voltage; I_{Kr}, rapidly activating delayed rectifier K current; I_{Ks}, slowly activating delayed rectifier K current; Hsp, heat-shock protein; LQTS, long QT syndrome; E4031, 1-[2-(6-methyl-2-pyridyl)-ethyl]-4-(4-methylsulfonylaminobenzoyl)piperdine.

To our surprise, we found that As_2O_3 produced its effects not by direct block of cardiac ion channels, but indirectly, by increasing cardiac calcium currents and by inhibiting the processing of hERG protein in the endoplasmic reticulum (ER). This report represents the first example of drug-induced LQTS in which an acquired trafficking defect of a cardiac ion channel contributes to QT prolongation and TdP.

Materials and Methods

Western Blot Analysis. Stable cell lines and antibodies used in the present study have been described previously (Ficker et al., 2003). Cells were solubilized for 1 h at 4°C in a lysis buffer containing 1% Triton X-100 and protease inhibitors (Complete; Roche Diagnostics, Indianapolis, IN). Protein concentrations were determined by the bicinchoninic acid method (Pierce Chemical, Rockford, IL). Proteins were separated on SDS polyacrylamide gels, transferred to polyvinylidene difluoride membranes, and developed using appropriate antibodies and ECL Plus (Amersham Biosciences, Piscataway, NJ). For quantitative analysis, chemiluminescence signals were captured directly on a Storm PhosphorImager (Amersham Biosciences) (Ficker et al., 2003).

Metabolic Labeling and Immunoprecipitation. HEK/hERG WT cells were starved for 30 min and pulse-labeled for 60 min in 100 to 150 μCi/ml [^{35}S]methionine/cysteine-containing medium. Cells were treated for 5 min at room temperature with 2 mM of the chemical cross-linker dithiobis(succinimidyl propionate) (Pierce Chemical). Cross-linking was quenched by the addition of glycine. Cells were harvested and lysed in a 0.1% Nonidet P-40 buffer in the presence of protease inhibitor (Ficker et al., 2003). Immunoprecipitation reactions were incubated overnight at 4°C and collected with Protein G Dynabeads (Dynal Biotech, Lake Success, NY). Samples were boiled in β-mercaptoethanol/SDS sample buffer to reverse cross-linking and to release immunoprecipitated proteins. Eluted samples were separated by SDS-polyacrylamide gel electrophoresis and analyzed with a Storm PhosphorImager (Amersham Biosciences) (Ficker et al., 2003).

In pulse-chase experiments performed without chemical cross-linking, image densities of fully and core-glycosylated hERG protein bands were determined after different chase periods by integrating pixel densities from equal areas after background subtraction. Image densities were normalized to the signal of the freshly synthesized, core-glycosylated hERG protein band isolated immediately after radiolabeling at $t = 0$. Pulse-chase data represent measurements from at least three independent experiments and are shown as mean ± S.E. After normalization, the time course of protein degradation as well as generation of fully glycosylated hERG protein can be compared directly between different experiments.

To quantify hERG/chaperone interactions at specific time points, image densities of core-glycosylated hERG protein bands were determined on autoradiograms after immunoprecipitation with anti-hERG, anti-Hsp90, and anti-Hsp/c70 antibodies as described. Image densities found in immunoprecipitations with anti-hERG antibody were used as a measure of total hERG protein present. Image densities of hERG protein bands isolated with antichaperone antibodies were normalized to image densities of hERG protein bands isolated with anti-hERG antibody to compute association quotients, which were used to assess time-dependent changes in hERG-chaperone

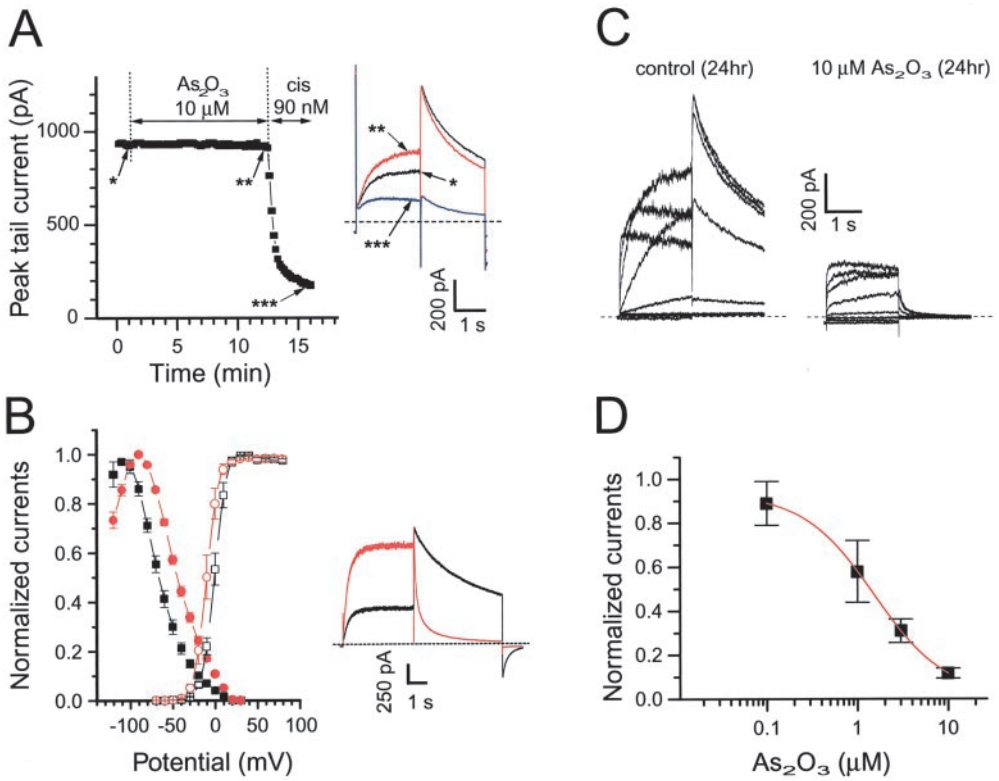

Fig. 1. Long-term exposure to As_2O_3 reduces the cardiac potassium current hERG stably expressed in HEK293 cells. A, left, hERG tail currents are not affected by short-term, extracellular application of 10 μM As_2O_3 but are reduced by the hERG blocker cisapride. Right, hERG currents recorded under control conditions (⋆), in 10 μM As_2O_3 (⋆⋆), and in cisapride (⋆⋆⋆). Currents were elicited from an HP of −80 mV with depolarizing voltage pulses to +20 mV. Tail currents were recorded on return to −50 mV. Note that short-term application of As_2O_3 increased hERG current during the depolarizing test pulse. B, left, steady-state inactivation and activation curves recorded under control conditions (■ and □) and after 3-h exposure to 3 μM As_2O_3 (● and ○). Right, hERG currents recorded under control conditions and after 3-h exposure to 3 μM As_2O_3 using the voltage protocol described in A. For comparison, an overlay is shown of a control and an As_2O_3-treated HEK/hERG cell expressing similar current levels. C, hERG currents recorded under control conditions and after overnight exposure (24 h) to 10 μM As_2O_3 using depolarizing voltage steps (HP = −80 mV). D, concentration-dependent reduction of hERG tail current amplitudes by overnight exposure to As_2O_3. IC_{50} is 1.5 μM (n = 6–7).

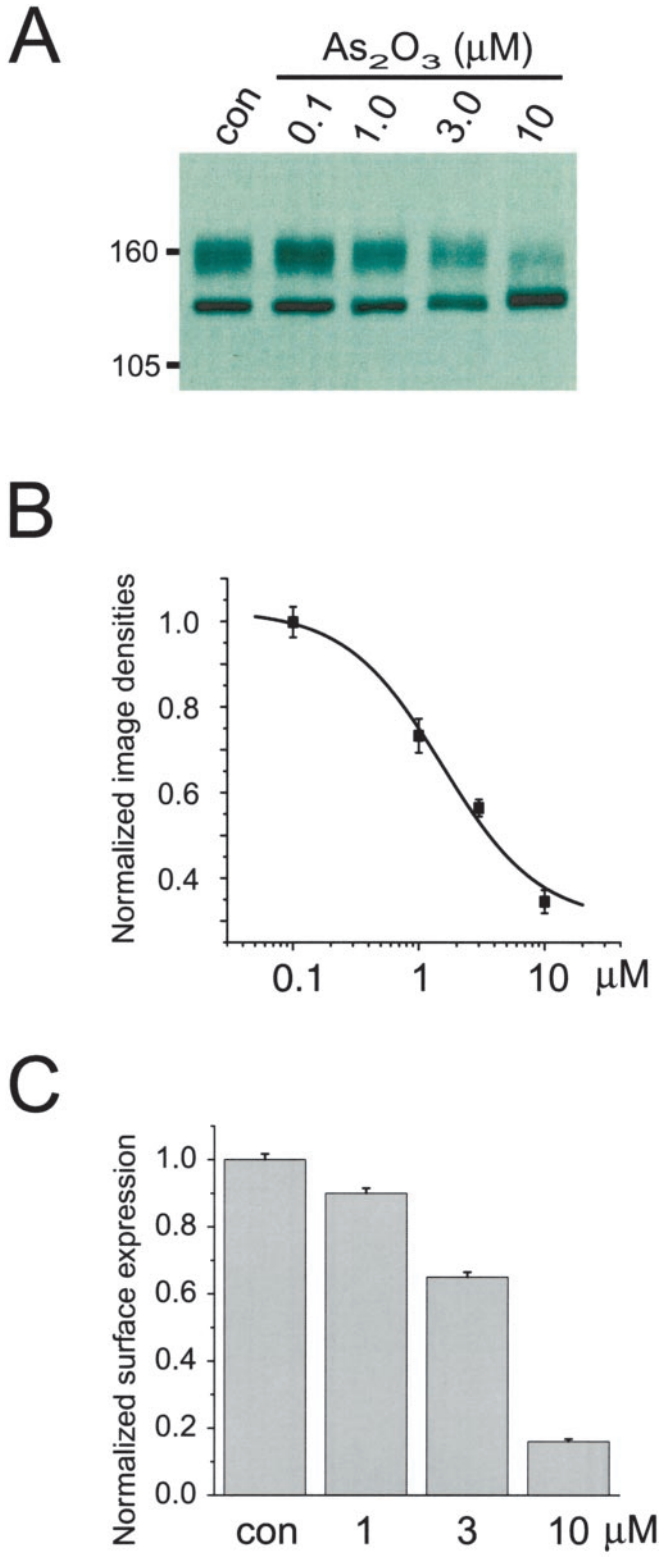

Fig. 2. As_2O_3 inhibits maturation and surface expression of hERG. A, Western blot showing effects of overnight exposure to increasing concentrations of As_2O_3 on hERG WT protein stably expressed in HEK293 cells. B, concentration-dependent reduction of fully glycosylated 155-kDa hERG on Western blots after overnight exposure to As_2O_3. IC_{50} is 1.5 μM (n = 4). Image densities on Western blots were analyzed directly on a Storm PhosphorImager. C, overnight exposure to As_2O_3 reduces in a concentration-dependent manner surface expression levels of HA_{ex}-tagged hERG protein stably expressed in HEK293 as determined by chemiluminesence measurements (n = 6).

interactions independently from small variations between different experiments. Data are shown as mean ± S.E. of three independent experiments.

Chemiluminescence Detection of Cell Surface hERG Protein. A hemagglutinin (HA) tag was inserted into the extracellular loop of hERG between transmembrane domains S1 and S2 (Ficker et al., 2003). Stably transfected HEK/hERG WT HA_{ex} cells were plated at 40,000 cells/well in a 96-well plate. After overnight incubation with As_2O_3, cells were fixed with ice-cold 4% paraformaldehyde, blocked by incubation with 1% goat serum, and incubated for 1 h with rat anti-HA antibody (Roche Diagnostics). After washing, horseradish peroxidase-conjugated goat anti-rat IgG (Jackson ImmunoResearch Laboratories Inc., West Grove, PA) and the double-stranded DNA stain SYBR Green (Molecular Probes, Eugene, OR) were added for 1 h (Myers, 1998; Margeta-Mitrovic et al., 2000). SYBR Green fluorescence was measured to determine cell numbers, after which chemiluminescent signals were developed using Super-Signal (Pierce Chemical) and captured in a luminometer. Luminescence signals in As_2O_3-treated wells were corrected for cell loss as measured by SYBR Green fluorescence with the data presented as normalized surface expression relative to control. For correction of cell loss, a standard curve of SYBR Green fluorescence was generated using four different amounts of cells per well (10, 20, 30, or 40 × 10^3, n = 3). Chemiluminescence signals were corrected when cell loss ranged from 10 to 75%.

Patch-Clamp Recordings. HEK/hERG WT and L/hKv1.5 cells were recorded using patch pipettes filled with 100 mM K-aspartate, 20 mM KCl, 2 mM $MgCl_2$, 1 mM $CaCl_2$, 10 mM EGTA, and 10 mM HEPES, pH 7.2. The extracellular solution was 140 mM NaCl, 5 mM KCl, 1 mM $MgCl_2$, 1.8 mM $CaCl_2$, 10 mM HEPES, and 10 mM glucose, pH 7.4. To study the long-term effects of As_2O_3 on hERG or Kv1.5 currents, drug was added to cell lines for 16 to 20 h (overnight) before recording. I_{Kr} and I_{Ks} currents and action potentials were recorded in ventricular guinea pig myocytes cultured overnight in M199 medium using the following intracellular solution: 119 mM K-gluconate, 15 mM KCl, 3.75 mM $MgCl_2$, 5 mM EGTA, 5 mM HEPES, 4 mM K-ATP, 14 mM phosphocreatine, 0.3 mM Tris-GTP, and 50 U/ml creatine phosphokinase, pH 7.2. The extracellular solution was 132 mM NaCl, 4 mM KCl, 1.2 mM $MgCl_2$, 1.8 mM $CaCl_2$, and 5 mM HEPES, pH 7.4. L-type Ca^{2+} currents were blocked with 1 μM nisoldipine. The specific hERG/I_{Kr} blocker E4031 was used to isolate I_{Kr} currents. Cardiac sodium currents were recorded using the following extracellular solution: 40 mM NaCl, 55 mM *N*-methyl-D-glucamine, 20 mM CsCl, 5.4 mM KCl, 2 mM $MgCl_2$, 0.02 mM $CaCl_2$, 30 mM TEA Cl, 5 mM 4-aminopyridine, and 10 mM HEPES, pH 7.4. The intracellular solution was 120 mM CsCl, 2 mM $MgCl_2$, 1 mM $CaCl_2$, 11 mM EGTA, 10 mM HEPES, 10 mM glucose, and 1 mM Mg-ATP, pH 7.2. Cardiac calcium-current traces were recorded using the following extracellular solution: 137 mM NaCl, 5.4 mM CsCl, 1.8 mM $MgCl_2$, 1.8 mM $CaCl_2$, 10 mM glucose, and 10 mM HEPES, pH 7.4. The intracellular solution was 130 mM Cs $MeSO_4$, 20 mM TEA Cl, 1 mM $MgCl_2$, 10 mM EGTA, 10 mM HEPES, 4 mM Mg-ATP, 14 mM Tris-phosphocreatine, 0.3 mM Tris-GTP, and 50 U/ml creatine phosphokinase, pH 7.2. To analyze current densities, membrane capacitances were measured using the analog compensation circuit of an Axon 200B patch-clamp amplifier (Axon Instruments Inc., Union City, CA). pCLAMP software (Axon Instruments) was used for generation of voltage-clamp protocols and data acquisition. All current recordings were performed at room temperature (20–22°C).

Results

Arsenic Trioxide Inhibits Maturation of the Cardiac Potassium Channel hERG. During treatment of patients with APL, As_2O_3 concentrations peak rapidly between 5 and 10 μM immediately after drug administration before reaching lower steady-state levels between 0.1 and 1 μM, the

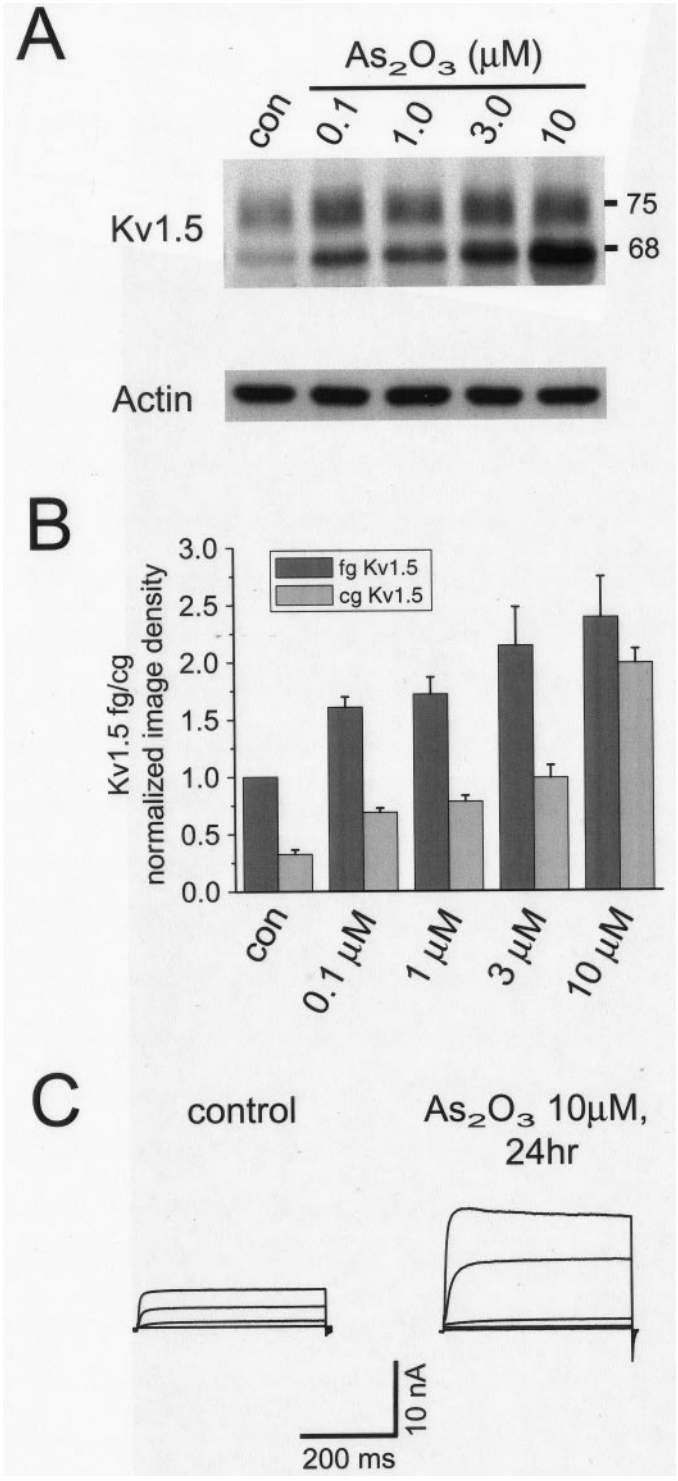

Fig. 3. As_2O_3 increases surface expression of the delayed rectifier potassium channel hKv1.5. A, steady-state levels of stably expressed hKv1.5 protein were determined by Western blotting upon overnight exposure to increasing concentrations of As_2O_3. HKv1.5 is expressed as a fully glycosylated protein of approximately 75 kDa and as a core-glycosylated protein of approximately 68 kDa. Actin was used as loading control. B, image densities of fully glycosylated and core-glycosylated hKv1.5 protein were quantified as a function of increasing As_2O_3 concentrations using a PhosphorImager and normalized to the fully glycosylated 75-kDa protein form measured under control conditions ($n = 4$). C, representative hKv1.5 currents recorded under control conditions and after overnight exposure (24 h) to 10 μM As_2O_3. Cells were held at −80 mV; test pulses were applied from −60 to +20 mV in increments of 20 mV.

therapeutically relevant concentration range (Shen et al., 1997). Neither 10 nor 100 μM As_2O_3 applied extracellularly reduced hERG tail current amplitudes recorded within 10 to 15 min (Fig. 1A). To exclude the possibility that access of As_2O_3 to an intracellular blocking site was hindered, we added 10 μM As_2O_3 to the intracellular patch solution. hERG tail current amplitudes remained stable for up to 1 h after the start of the intracellular perfusion (data not shown). Rather than short-term block, As_2O_3 significantly increased hERG outward currents and accelerated current deactivation. As_2O_3-induced gating changes became more pronounced with longer exposure, and after 3 h, we found shifts in steady-state activation and inactivation of −8.9 and +21.7 mV, respectively (Fig. 1B). These changes were accompanied by faster activation kinetics. At +20 mV, we measured an activation time constant of 549 ± 107 ms in control myocytes and 301 ± 94 after 3-h exposure to As_2O_3 ($n = 5$). The accelerated activation time course together with the depolarizing shift of the steady-state inactivation curve are responsible for the increase in hERG outward currents observed during 2-s depolarizations. Current deactivation was fit with two exponential time constants that decreased at −50 mV from 526 ± 54 and 2738 ± 271 ms in control myocytes to 155 ± 32 and 938 ± 80 ms after 3-h exposure, whereas tail current amplitudes were not affected (Fig. 1B; $n = 5$). Inactivation kinetics remained unchanged (data not shown).

Because As_2O_3 did not block hERG directly and gating changes were complex, we considered the possibility of an As_2O_3-induced trafficking block, as we have reported previously for geldanamycin (Ficker et al., 2003). We exposed stably transfected HEK/hERG cells overnight to increasing concentrations of As_2O_3 and tested for effects on hERG processing. First, we found that hERG current was reduced in a concentration-dependent manner with an IC_{50} of 1.5 μM as measured by analyzing tail current amplitudes on return to −50 mV after maximal activation with depolarizing voltage steps to +60 mV (Fig. 1, C and D). Second, we performed a Western blot analysis to test for changes in expression of hERG protein (Fig. 2A). It is known that hERG channels are synthesized in two forms: 1) an immature core-glycosylated protein of approximately 135 kDa that is localized to the ER, and 2) a fully glycosylated mature protein of approximately 155 kDa, which is transported to the cell surface (Zhou et al., 1998). Incubation with As_2O_3 for 24 h produced a time- and concentration-dependent decrease in the amount of mature, fully glycosylated hERG protein. Production of the fully glycosylated cell surface form of hERG was suppressed with an IC_{50} of 1.5 μM, identical with the long-term effect on currents (Fig. 2B). At higher concentrations of As_2O_3, hERG channels were primarily present as the ER resident 135-kDa form.

The equivalent effects on hERG current and fully glycosylated protein suggested that surface expression of hERG was suppressed. To examine changes in surface expression, we used a chemiluminescence assay. HEK293 cells stably expressing hERG with an extracellular HA epitope tag inserted in the extracellular S1 to S2 loop (Ficker et al., 2003) were treated overnight with As_2O_3. As_2O_3 treatment caused a significant concentration-dependent reduction in hERG surface expression in line with the electrophysiological and biochemical experiments (Fig. 2C).

To examine the specificity of the As_2O_3 effects, we performed Western blot experiments with human Kv1.5 chan-

nels stably expressed in L cells. HKv1.5 channels are responsible for the ultra-rapid, delayed rectifier current found primarily in atrial myocytes (Nerbonne, 2000). The channel is synthesized as a core-glycosylated protein of approximately 68 kDa and matures into a fully glycoslyated cell surface protein of approximately 75 kDa (Ficker et al., 2003). When L/hKv1.5 cells were treated under steady-state conditions with As_2O_3, we detected a concentration-dependent increase in the fully glycosylated cell surface as well as the core-glycosylated protein form of hKv1.5 on Western blots (Fig. 3, A and B). The increase in surface expression was also reflected in electrophysiological experiments in which current densities increased significantly from 103.3 ± 25.9 pA/pF at 0 mV ($n = 8$) measured under control conditions to 733.8 ± 246.5 pA/pF ($n = 5$, $p < 0.05$, Student's t test) after overnight exposure to 10 μM As_2O_3 (Fig. 3C). In addition, we studied Kv4.3, the channel responsible for the cardiac transient outward current (Nerbonne, 2000) and found that current densities were not altered after incubation with As_2O_3 (data not shown).

Mechanism of hERG Suppression by As_2O_3. To explore the effects of As_2O_3 on hERG processing more directly, we performed pulse-chase experiments (Fig. 4A). Measured immediately after radiolabeling ($t = 0$ h), similar quantities of ER-resident, 135-kDa hERG were synthesized under control conditions and after preincubation with 3 μM As_2O_3. In control myocytes, within the first 6 h, approximately 50% of the initially synthesized 135-kDa protein progressed to the

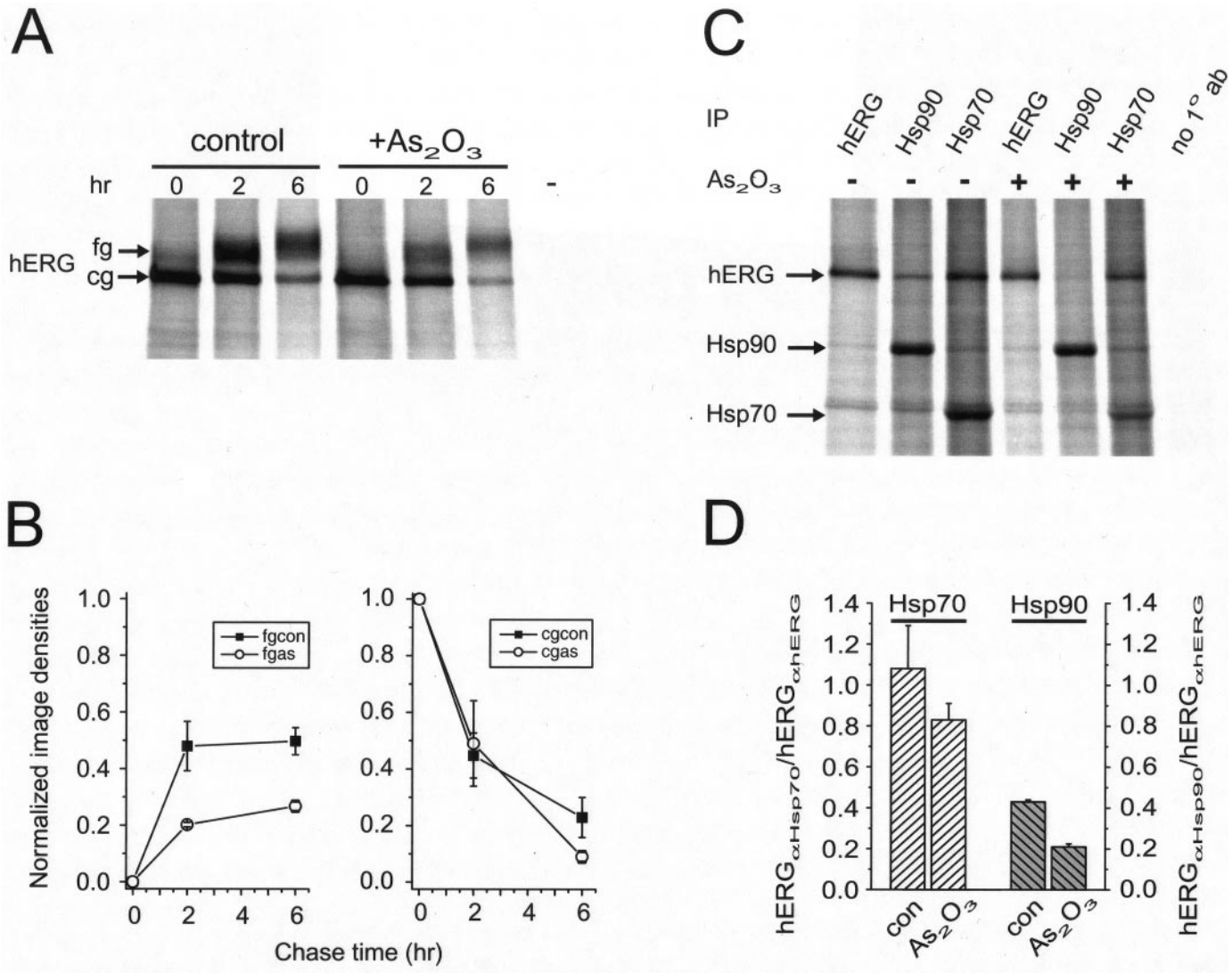

Fig. 4. As_2O_3 inhibits the progression of core-glycosylated hERG into the fully glycosylated form. A, radiolabeled hERG protein was isolated immediately after synthesis (t = 0) or after the chase periods indicated (t = 2 and 6 h) under control conditions or after overnight exposure to 3 μM As_2O_3. Right lane, control with no primary antibody present. Arrows indicate position of core- (cg) and fully glycosylated (fg) hERG. B, normalized image densities for fg- (left) and cg-hERG (right) shown as functions of chase time in the absence (fg/cgcon) and presence of 3 μM As_2O_3 (fg/cgas, $n = 3$). C, analysis of hERG/chaperone complexes formed under control conditions and in the presence of 3 μM As_2O_3. Radiolabeled hERG/chaperone complexes were isolated immediately after synthesis by immunoprecipitation with anti-hERG, anti-Hsp90, and anti-Hsp70 antibodies and resolved on SDS-polyacrylamide gel electrophoresis. Right lane, control with no primary antibody added. Arrows indicate position of the respective protein bands. D, quantitative analysis of As_2O_3-induced changes in hERG/chaperone association. Image densities of core-glycosylated 135-kDa hERG protein bands were quantified after immunoprecipitation using a Storm PhosphorImager. hERG image densities determined for immunoprecipitations with anti-Hsp/c70 and anti-Hsp90 were normalized to densities found in immunoprecipitations with anti-hERG antibody used as measure of total hERG protein. Normalized mean values of hERG association with either Hsp70 or Hsp90 are shown for controls and for samples exposed overnight to 3 μM As_2O_3 ($n = 3$).

mature, fully glycosylated 155-kDa form. When HEK/hERG cells were pretreated with 3 μM As_2O_3 for 16 h before the pulse-chase experiment, maturation of the ER-resident form was reduced to approximately 25%, consistent with our steady-state experiments (Fig. 4B).

Because the cytosolic chaperones Hsp70 and Hsp90 are required for the biochemical maturation of hERG (Ficker et al., 2003), we determined whether As_2O_3 reduced steady-state expression levels of endogenous Hsp90 and/or Hsp70. Neither Hsp90 nor Hsp70 levels were significantly altered after overnight exposure to 3 μM As_2O_3 (data not shown). Because the trafficking block observed with As_2O_3 was reminiscent of effects induced by geldanamycin and radicicol, two specific inhibitors of Hsp90 (Roe et al., 1999; Ficker et al., 2003), we tested next whether As_2O_3 modified the association of hERG channels with Hsp70 and/or Hsp90 in coimmunoprecipitation experiments using a stable HEK/hERG WT cell line and radiolabeling to determine the formation of channel/chaperone complexes. After radiolabeling, hERG WT was immunoprecipitated in its core-glycosylated 135-kDa form using anti-hERG antibody. When the formation of hERG-Hsp70 chaperone complexes was assessed in immunoprecipitations with anti-Hsp/c70 antibody, we found Hsp70 in complex with newly synthesized, 135-kDa hERG protein (Fig. 4C). Likewise, Hsp90 could be isolated under control conditions in complex with the 135-kDa form of hERG. However, in the presence of As_2O_3, the formation of hERG/Hsp90 complexes was inhibited by approximately 50%, whereas the formation of hERG/Hsp70 complexes was reduced by approximately 20% (Fig. 4D). Taken together, these data provide evidence that the arsenic-induced trafficking block of hERG is probably caused by altered channel/chaperone interactions.

Arsenic Trioxide Reduces Native I_{Kr} Currents in Guinea Pig Ventricular Myocytes. To test whether our analysis in heterologous expression systems may be extended to ventricular cardiomyocytes, we first studied the effects of extracellularly applied As_2O_3 on action potentials evoked in freshly isolated guinea pig ventricular myocytes. We found that action potential duration (APD) was not affected by

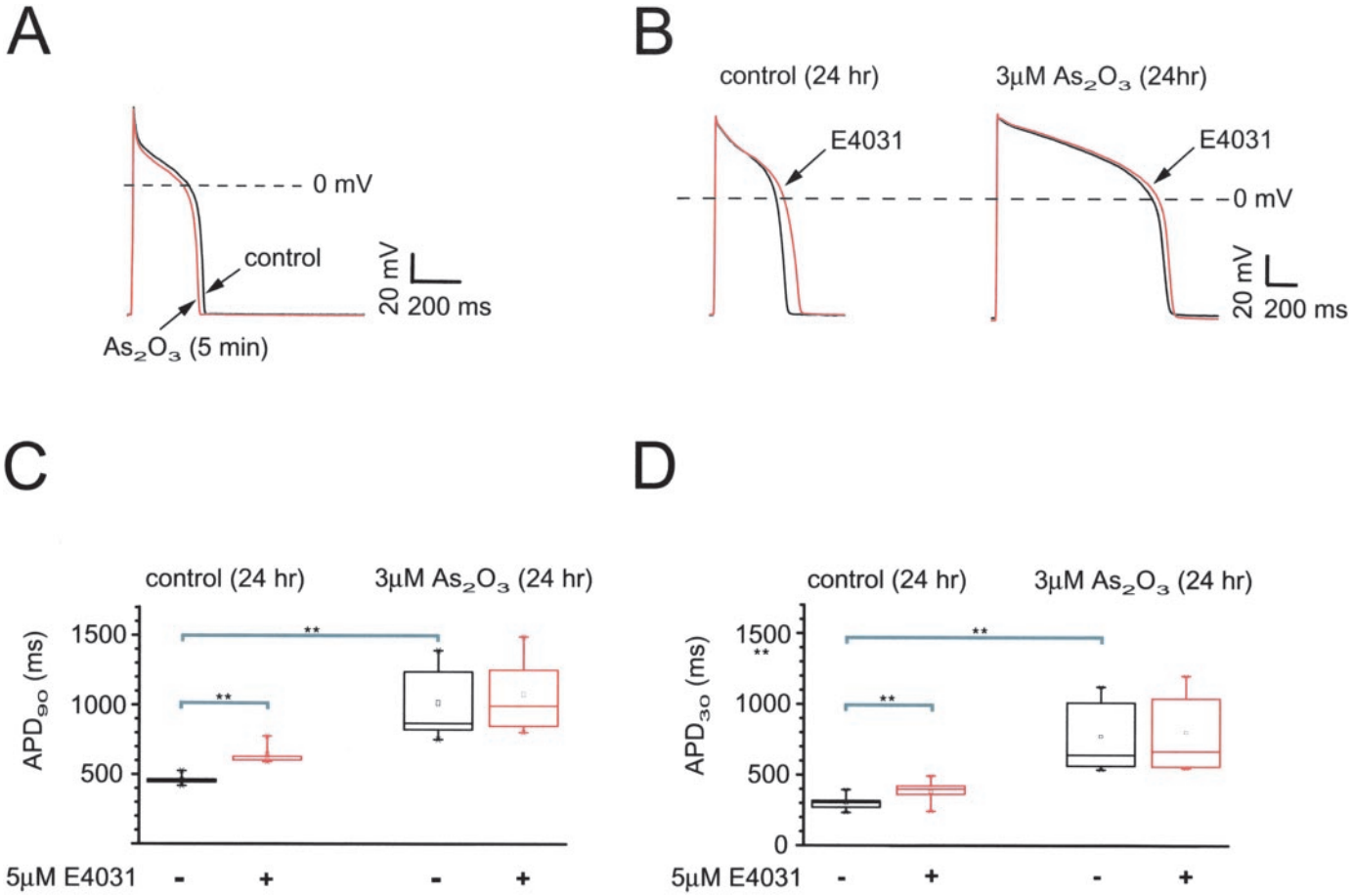

Fig. 5. Overnight exposure to As_2O_3 prolongs the cardiac action potential in guinea pig ventricular myocytes. A, current clamp recordings of action potentials (AP) elicited in a freshly isolated ventricular myocyte under control conditions and 5 min after start of extracellular perfusion with 3 μM As_2O_3 (red trace). Membrane potential (MP) was -80 mV. B, left, APs elicited in the absence and presence of 5 μM E4031 (red trace) in a ventricular myocyte cultured overnight (24 h) under control conditions. Right, cardiac APs elicited in the absence and presence of 5 μM E4031 (red trace) in a myocyte cultured overnight in medium containing 3 μM As_2O_3. MP was -80 mV. C, quantitative analysis of APD_{90} under control conditions and after exposure to 3 μM As_2O_3. E4031 (5 μM) was used to determine prolongation of cardiac action potentials on blockade of native I_{Kr}/hERG currents (n = 5–6). APD_{90} was significantly prolonged in myocytes cultured overnight with 3 μM As_2O_3 (Student's t test, $\star\star$, $p < 0.05$). hERG block by E4031 prolonged the cardiac action potentials only in myocytes cultured under control conditions (Student's t test, $\star\star$, $p < 0.05$). Data are represented as statistical box charts with asterisk representing outliers, whiskers determining the 5th and 95th percentiles, and boxes determining the 25th and 75th percentiles. Means are represented by □. D, quantitative analysis of APD_{30} under control conditions and after exposure to 3 μM As_2O_3. E4031 (5 μM) was used to block hERG currents (n = 5–6). APD_{30} was significantly prolonged in myocytes cultured overnight in the presence of 3 μM As_2O_3. $\star\star$, significance at $p < 0.05$ level as determined with Student's t test. Data are represented as statistical box charts.

short-term As_2O_3 application (Fig. 5A). However, when myocytes were cultured overnight under control conditions or in the presence of 3 μM As_2O_3, APD_{90} was significantly prolonged from 459 ± 15 to 1014 ± 127 ms, respectively (n = 5–6) (Fig. 5, B and C). Because our experiments in heterologous expression systems pointed toward hERG/I_{Kr} as the target for prolongation of APD_{90}, we used the specific blocker E4031 to evaluate the contribution of hERG/I_{Kr} currents to cardiac repolarization under control conditions and after overnight treatment with 3 μM As_2O_3. In these experiments, E4031 significantly prolonged APD_{90} by 179 ± 34 ms under control conditions, whereas in As_2O_3 treated myocytes, APD_{90} was not affected (Fig. 5C). Similar changes were observed in APD_{30}, a measure of repolarization more geared toward changes in depolarizing inward currents, with APD_{30} increasing from 301 ± 22 to 774 ± 122 ms upon overnight exposure of myocytes to 3 μM As_2O_3.

Because experiments with E4031 indicated that a reduction of hERG/I_{Kr} currents may underlie the prolonged action potentials in As_2O_3-treated myocytes, we analyzed current densities of the cardiac rapid, delayed rectifier current I_{Kr} in voltage-clamp experiments. I_{Kr} currents were elicited during 650-ms depolarizations from a holding potential (HP) of −40 mV in cultured guinea pig cardiomyocytes treated overnight with 1.5 or 3 μM As_2O_3. I_{Kr} was isolated as an E4031-sensitive tail current upon return from +60 mV (Fig. 6, A and B1). As_2O_3 (1.5 and 3 μM) reduced tail current densities in guinea pig cardiomyocytes from 0.7 to 0.3 and 0.03 pA/pF,

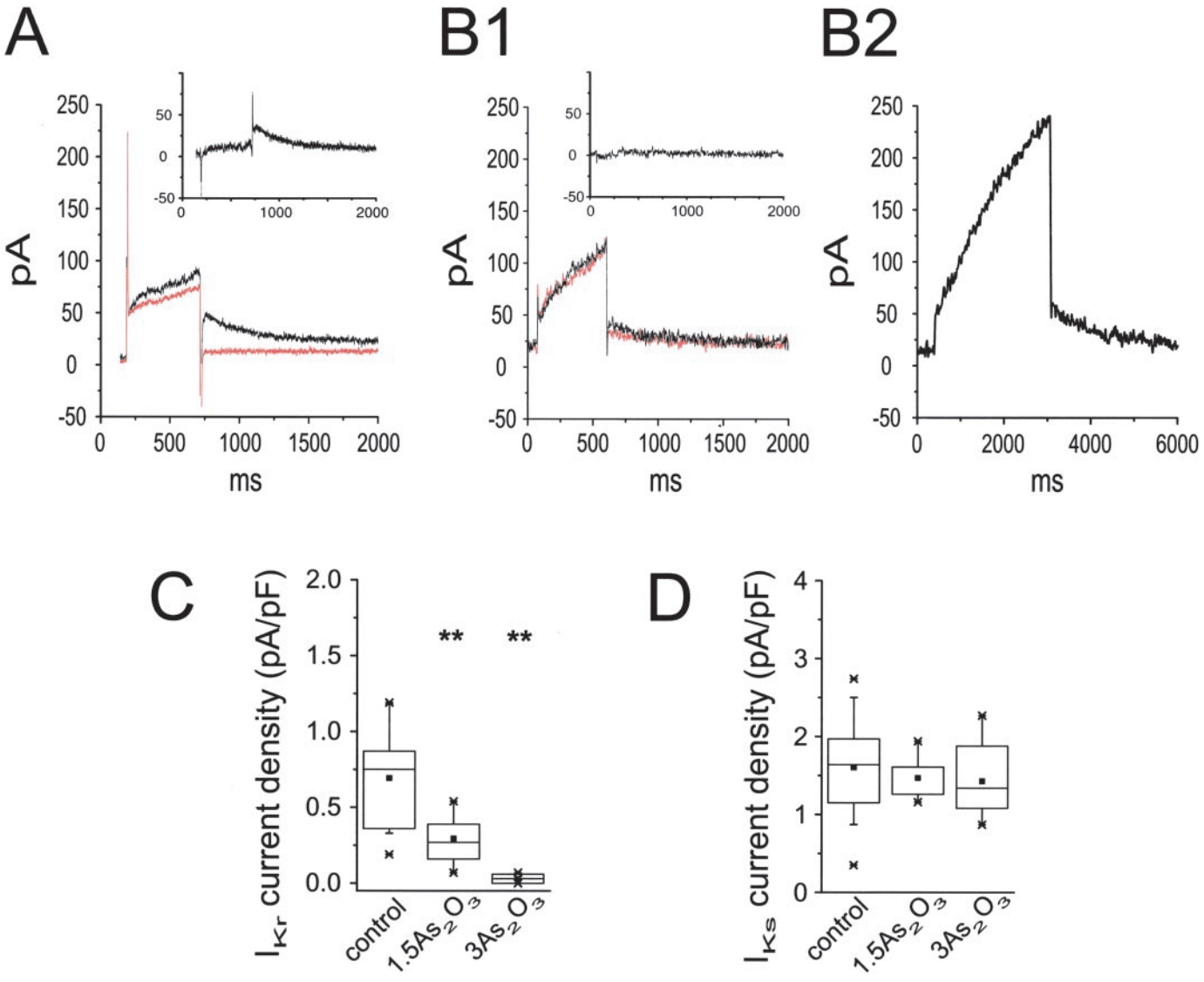

Fig. 6. As_2O_3 reduces amplitudes of native I_{Kr}/hERG currents in cultured guinea pig ventricular myocytes. A, isolation of E4031-sensitive I_{Kr} current in a ventricular myocyte cultured overnight under control conditions. Current traces were elicited with a voltage step to +60 mV from an HP of −40 mV in the absence and presence of 5 μM E4031 (red trace). Cell capacitance was 55 pF. Inset, E4031-sensitive I_{Kr} current component was isolated by subtraction of outward current recorded in the presence of E4031 from control current. B1, outward currents elicited in the absence and presence of 5 μM E4031 (red trace) in a ventricular myocyte cultured overnight in medium containing 3 μM As_2O_3. Voltage protocol was performed as described in A. Cell capacitance was 64 pF. Inset, subtraction current isolated from currents recorded in E4031 and under control conditions. B2, slow, delayed rectifier current I_{Ks} measured with 2.5-s voltage steps to +60 mV in the presence of 5 μM E4031. Same cell shown as in B1. I_{Ks} currents were identified as E4031-resistant tail currents upon return to −40 mV. C, I_{Kr} current densities measured after overnight culture in control myocytes (n = 14) and in myocytes treated with either 1.5 (n = 9) or 3 μM As_2O_3 (n = 6). Current densities are represented in statistical box charts and were significantly smaller in As_2O_3-treated myocytes (analysis of variance followed by Dunnett's test; ⋆⋆, $p < 0.05$). D, analysis of I_{Ks} current densities in control myocytes (n = 16) and in myocytes treated with either 1.5 (n = 8) or 3 μM As_2O_3 (n = 7).

respectively (Fig. 6C). To test for specificity, slow, delayed rectifier currents I_{Ks} were elicited in the presence of 5 μM E4031 with 2.5-s step depolarizations (Fig. B2) and were not changed by drug exposure (Fig. 6D). Our data show that processing and maturation of cardiac I_{Ks} channels are not sensitive to As_2O_3 and reveal specificity in the interaction of As_2O_3 with different potassium channels. In addition, current densities of the cardiac inward rectifier current I_{K1} did not change upon long-term exposure to As_2O_3. At -100 mV, we measured 12.0 $\pm$ 0.8 pA/pF under control conditions and 11.0 $\pm$ 0.7 pA/pF after overnight exposure to 3 μM As_2O_3 (n = 5).

Arsenic Trioxide Increases Cardiac Calcium Currents in Ventricular Myocytes. Because our analysis of APD_{30} pointed toward the participation of depolarizing inward currents in As_2O_3-induced prolongation of cardiac repolarization, we also studied cardiac sodium and calcium currents. Sodium currents were elicited using a short depolarizing pulse protocol after a conditioning prepulse to -140 mV (Fig. 7A). I-V relationships recorded in control myocytes versus myocytes exposed overnight to As_2O_3 showed a shift in the activation of sodium currents to more hyperpolarized potentials and a modest increase in current density (Fig. 7B). To analyze potential changes in inactivation kinetics and late current amplitudes, we applied As_2O_3 to HEK293 cells stably expressing the human cardiac Na^+ channel gene SCN5A. Neither parameter was affected by As_2O_3 (data not shown).

In contrast to the small changes in cardiac sodium currents, cardiac calcium current density more than doubled, from -5.2 ± 0.7 pA/pF (n = 6) in control myocytes at 0 mV to -17.7 ± 1.3 pA/pF (n = 10) in ventricular myocytes exposed overnight to 3 μM As_2O_3 (Fig. 7, C and D). The increase in current density was accompanied by small changes in the voltage-dependence of activation and an acceleration of the rate of inactivation. The large changes in calcium current are expected to prolong the cardiac action potential independent of the reported reduction of hERG/I_{Kr} currents. To demonstrate the contribution of calcium currents to the prolongation of cardiac action potentials, we used 25 nM nisoldipine, which shortened APD_{90} from 880 $\pm$ 61 ms in myocytes treated overnight with 3 μM As_2O_3 to 686 $\pm$ 36 ms. The latter is close to APD_{90} values of 495 $\pm$ 40 ms measured under control conditions (Fig. 8; n = 4). At a much higher concentration of 1 μM nisoldipine, APD_{90} was further shortened to 254 $\pm$ 15 ms in control myocytes and to 304 $\pm$ 12 ms in myocytes incubated overnight with 3 μM As_2O_3 (Fig. 8; n = 4). The longer APD_{90} values measured in As_2O_3-treated myocytes are consistent with inhibition of hERG/I_{Kr} trafficking.

Short-Term Effects of Arsenic Trioxide. Modifications of hERG/I_{Kr} currents by As_2O_3 proceed in two different time windows: 1) gating changes that occur in minutes, and 2) changes in surface expression that occur in hours and are caused by alterations in protein processing. To study time-dependent changes of cardiac calcium currents closely, we analyzed current densities in myocytes exposed for short

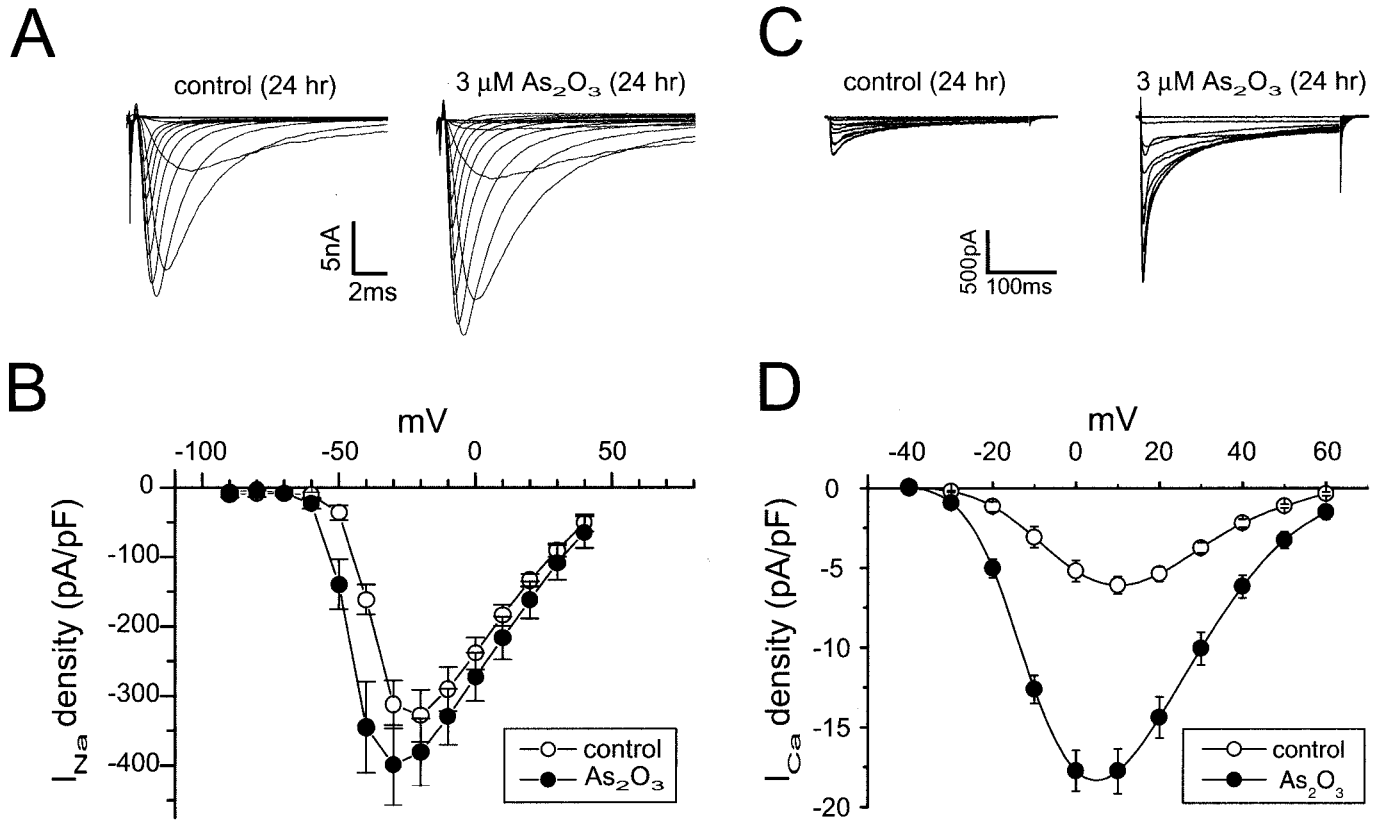

Fig. 7. As_2O_3 increases cardiac calcium currents. A, effect of As_2O_3 treatment on Na^+ currents in cultured guinea pig ventricular myocytes. Current traces were elicited using 20-ms depolarizations in increments of 10 mV (500-ms prepulse to -140 mV; HP = -80 mV) in ventricular myocytes cultured overnight (24 h) in the absence or presence of 3 μM As_2O_3. B, averaged I-V relationships (n = 6–10). C, effect of As_2O_3 on cardiac calcium currents in cultured guinea pig ventricular myocytes. Current traces were elicited using 300-ms step depolarizations in increments of 10 mV (HP = -40 mV) in myocytes cultured overnight (24 h) in the absence and presence of 3 μM As_2O_3. D, averaged I-V relationships (n = 12–16).

times to 3 μM As_2O_3. We found a small increase in cardiac calcium current density after a 1-h exposure (Fig. 9A). At the same time, APD_{90} was prolonged from 581 ± 18 to731 ± 65 ms (n = 5–6) (Fig. 9, C and D). After 3 h, calcium currents were further increased with APD_{90} prolonged from 494 ± 78 to 725 ± 68 ms (n = 8–13) (Fig. 9B). Because changes in surface expression of ion channels are a function of slow protein turnover rates, we speculated that the fast changes in cardiac repolarization seen after 1- and 3-h exposure to As_2O_3 may be caused either by fast gating changes in hERG currents and/or by the fast increase in calcium-current densities demonstrated in our experiments. To decide between these possibilities, we assayed the contribution of hERG/I_{Kr} currents to cardiac repolarization in myocytes exposed for 1 h to As_2O_3 using 5 μM of the specific hERG/I_{Kr} blocker E4031. We found that hERG/I_{Kr} contributed to a similar extent in both control and As_2O_3-treated myocytes. E4031 (5 μM) increased APD_{90} by 211 ± 18 ms in control and by 284 ± 32 ms in As_2O_3-treated myocytes (n = 5–6; ΔAPD_{90} values were not significantly different, Student's t test, $p < 0.05$) (Fig. 9D). Likewise, APD_{30} was increased after 1-h exposure to As_2O_3. However, E4031 increased APD_{30} by 205 ± 21 ms in As_2O_3-treated myocytes, whereas in control myocytes, APD_{30} was prolonged only by 85 ± 12 ms (n = 5–6; ΔAPD_{30} values significantly different at $p < 0.05$ level, Student's t test) (Fig. 9E). Hence, our analysis suggests that the contribution of hERG/I_{Kr} currents to cardiac repolarization was not altered by fast gating changes and that the prolongation of cardiac repolarization seen on initial exposure to As_2O_3 is most likely the result of an increase in calcium current amplitudes.

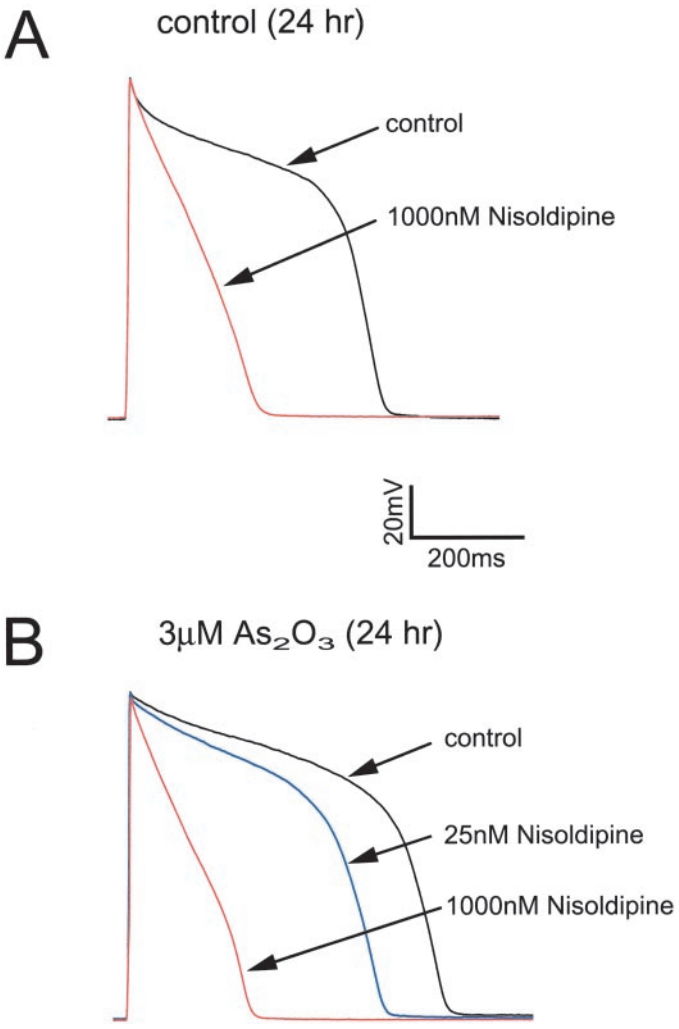

Fig. 8. The L-type calcium channel antagonist nisoldipine shortens cardiac action potentials prolonged by long-term exposure to As_2O_3. A, cardiac APs elicited in a ventricular myocyte cultured overnight (24 h) under control conditions and 5 min after start of extracellular perfusion with 1000 nM nisoldipine (red trace). MP was −80 mV. B, cardiac APs recorded in a ventricular myocyte cultured overnight in the presence of 3 μM As_2O_3 (24 h) and after perfusion with 25 (blue trace) or 1000 nM nisoldipine (red trace). MP was −80 mV.

Short-Term Effects of Membrane-Permeable Phenyl Arsine Oxide. Given our results with short-term incubations, it is surprising that As_2O_3 applied with the extracellular perfusate for up to 15 min was not able to produce short-term changes in cardiac action potentials recorded at room temperature (Fig. 5A). One explanation may be that the uptake of As_2O_3 into cardiac myocytes is slow at room temperature. To overcome slow uptake, we added 10 μM As_2O_3 to the intracellular patch solution and recorded cardiac action potentials. We found that 10 μM As_2O_3 applied for 10 min via the patch pipette prolonged APD_{90} in three of six cells from 616 ± 59 to 866 ± 98 ms and APD_{30} from 410 ± 31 to 641 ± 49 ms (n = 3; both APD_{90} and APD_{30} were significantly prolonged at $p < 0.05$, Student's t test). In marked contrast, both APD_{90} and APD_{30} were stable for more than 15 min after the start of intracellular perfusion with control solution (Fig. 10A). Thus, fast changes in cardiac calcium current seem to depend on the access of As_2O_3 to intracellular sites. In another test of fast modification of cardiac calcium currents, we applied the membrane-permeable As_2O_3 analog phenyl arsine oxide (PAO) with the extracellular perfusate. In electrophysiological experiments, PAO applied at 10 μM with the extracellular perfusate increased calcium-current amplitudes within minutes (Fig. 10B). At the same time, current inactivation kinetics became faster. Both changes in cardiac calcium currents were similar to what has been observed upon long-term exposure to As_2O_3. Taken together, our data suggest that calcium currents are modified in a fast process that is limited only by As_2O_3 gaining access to the sarcoplasm of cardiac ventricular myocytes.

Discussion

In the present study, we provide evidence that As_2O_3 prolongs the action potential of guinea pig ventricular myocytes via two independent molecular mechanisms. As_2O_3 increases cardiac calcium currents, which regulate the plateau phase of the cardiac action potential but also reduces surface expression of the cardiac potassium current hERG/I_{Kr}, which is crucial to later stages of cardiac repolarization. The effects on current amplitudes were preceded by changes in hERG gating kinetics induced immediately upon exposure to As_2O_3. Enhanced outward currents and accelerated deactivation kinetics have been reported as a hallmark of hERG modulation by radical oxygen species (ROS) (Taglialatela et al., 1997; Berube et al., 2001) and are compatible with the well-documented property of As_2O_3 to induce oxidative stress by increasing ROS production (Liu et al., 2001). However, ROS-induced gating changes of hERG are ambiguous in their effects on cardiac repolarization in that faster activating hERG currents allow for larger outward currents during the

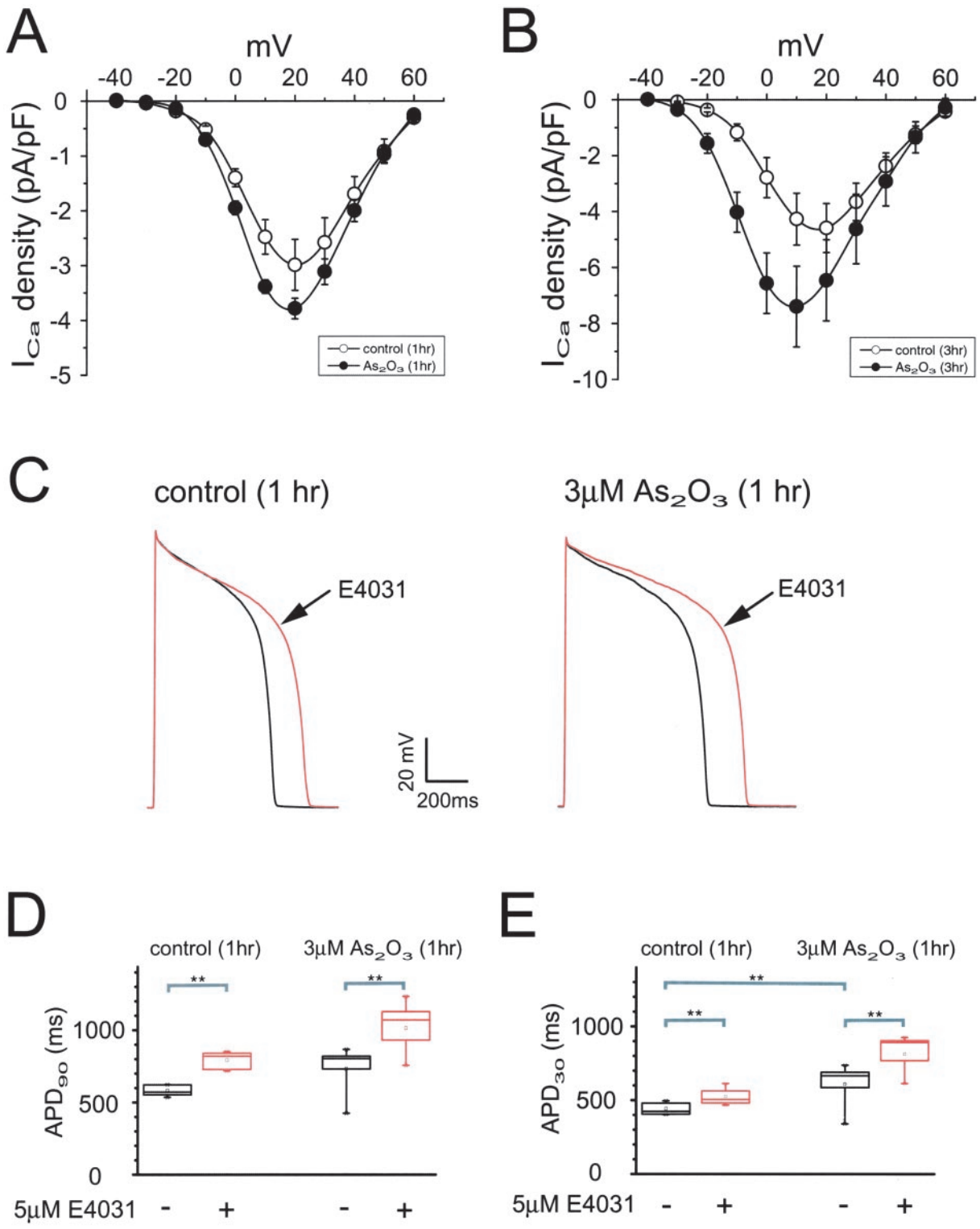

Fig. 9. Short time exposure of guinea pig ventricular myocytes to As_2O_3. A, changes in cardiac calcium currents induced by 1-h exposure to 3 μM As_2O_3. Averaged I-V relationships were determined from cardiac calcium currents elicited with 300-ms step depolarizations in increments of 10 mV from a holding potential of −40 mV in control myocytes and in myocytes treated for 1 h with 3 μM As_2O_3 (n = 6). B, effects of 3-h exposure to 3 μM As_2O_3 on cardiac calcium currents, and averaged I-V relationships (n = 7). C, left, cardiac APs elicited in the absence and presence of 5 μM E4031 (red trace) in a control myocyte cultured for 1 h. Right, cardiac APs elicited in the absence and presence of 5 μM E4031 (red trace) in a myocyte cultured for 1 h in medium containing 3 μM As_2O_3. MP was −80 mV. D, quantitative analysis of APD_{90} under control conditions and after 1-h exposure to 3 μM As_2O_3. E4031 was used to determine the contribution of hERG currents to cardiac repolarization. Data are represented as statistical box charts. APD_{90} was not significantly prolonged on 1-h incubation with 3 μM As_2O_3 when control myocytes were compared with myocytes treated for 1 h with 3 μM As_2O_3. ★★, significance at $p < 0.05$ level as determined with Student's t test. E, quantitative analysis of APD_{30} under control conditions and after 1-h exposure to 3 μM As_2O_3 (n = 5–6). E4031 was used to determine contribution of hERG currents to cardiac repolarization. Data are represented as statistical box charts. Note that APD_{30} was significantly different between control myocytes and myocytes treated for 1 h with 3 μM As_2O_3. ★★, significance at $p < 0.05$ as determined with Student's t test.

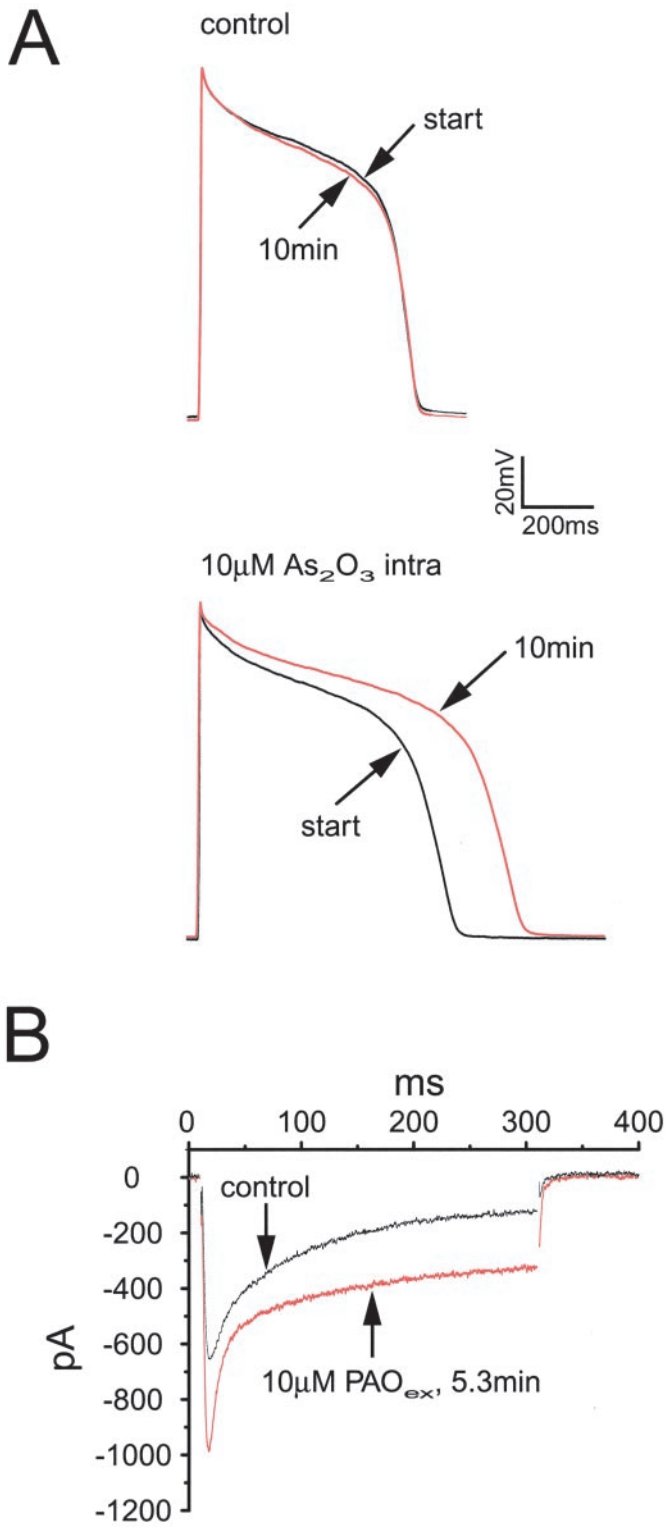

Fig. 10. Short-term effects of the membrane-permeable As_2O_3 analog PAO on cardiac calcium currents in freshly isolated guinea pig ventricular myocytes. A, top, cardiac APs elicited immediately after establishing whole-cell recording configuration and 10 min after start of perfusion with intracellular control solution in a freshly isolated myocyte. Bottom, cardiac APs elicited immediately after establishing whole-cell access and 10 min after start of perfusion with intracellular solution supplemented with 10 μM As_2O_3. MP was −80 mV; cycling time was 0.1 Hz. Although stable under control conditions, cardiac APs were prolonged with time on intracellular perfusion with 10 μM As_2O_3 in three of six freshly isolated myocytes. B, effects of extracellularly applied PAO. Cardiac calcium currents were elicited in freshly isolated myocytes with depolarizing voltage steps to +10 mV (HP = −40 mV, 0.1 Hz). PAO (10 μM) was applied with external perfusate while changes in current amplitude and kinetics were continuously monitored. Shown are typical calcium currents recorded under control conditions and 5.3 min after start of perfusion with 10 μM PAO. Note that observed changes mirror closely modifications of cardiac calcium currents observed on long-term exposure to As_2O_3.

plateau phase of the cardiac action potential with a tendency to shorten the cardiac action potential, whereas faster deactivation kinetics are expected to reduce hERG currents during cardiac repolarization and prolong the QT, as observed with As_2O_3. It is important the ROS-induced acceleration of current deactivation was not sufficient to prolong the cardiac action potential as judged from our current clamp experiments and seemed to be compensated by the concomitant ROS-induced increase in hERG outward currents. After 1-h exposure to As_2O_3, we detected an increase in cardiac calcium-current amplitudes accompanied by a prolongation of action potential duration. Changes in calcium current amplitudes became more pronounced with longer exposure times and seemed to be diminished in short-term experiments by slow uptake of As_2O_3 into the sarcoplasm. The changes in calcium currents were paralleled by an As_2O_3-induced block of hERG processing, which reduced hERG export to the cell surface. As expected, changes in cell-surface expression of hERG could be detected only after long-term exposure to As_2O_3 for several hours, because changes in surface expression are limited by the slow turnover rate of hERG channel protein of approximately 11 h (Ficker et al., 2003). Because patients are treated for several weeks with daily injections of As_2O_3, such a dosing regimen may be approximated best by long-term exposure of cardiomyocytes to As_2O_3.

Long-term exposure to As_2O_3 suppresses trafficking of hERG, and we propose that this mechanism underlies the reduction in I_{Kr} and the prolongation of action potential duration in ventricular myocytes. Trafficking block of hERG was observed at clinically relevant concentrations of 0.1 to 1.5 μM As_2O_3 (Shen et al., 1997). This report is the first to show acquired trafficking block as the basis for QT prolongation and TdP. It is consistent with other reports that electrocardiogram changes develop gradually and are observed most often after multiple rounds of treatment with As_2O_3 (Ohnishi et al., 2000; Unnikrishnan et al., 2001). It has been reported in guinea pig ventricular myocytes that cardiac action potential duration was significantly prolonged only with a delay of hours after feeding or intravenous infusion of As_2O_3; short-term effects were minimal (Chiang et al., 2002). Furthermore, a study in intact rabbits demonstrated long-term effects of As_2O_3 on cardiac action potential duration and QT interval that developed slowly over several weeks with no short-term effects reported (Wu et al., 2003).

Given the clinically available data (Ohnishi et al., 2000; Unnikrishnan et al., 2001), data from two different animal models (Chiang et al., 2002; Wu et al., 2003), and the present data acquired in stably transfected hERG/HEK cells, all of which point toward slow mechanisms of As_2O_3 action, it is surprising that short-term block of hERG and KvLQT/mink currents heterologously expressed in Chinese hamster ovary cells has been reported (Drolet et al., 2004). An explanation for the difference is not at hand. However, it is important to note that short-term application of As_2O_3 did not prolong action potential duration in guinea pig ventricular myocytes.

Moreover, long-term exposure to As_2O_3 blocked neither cardiac I_{Ks} nor I_{K1} currents. In addition, hERG/I_{Kr} current amplitudes were not altered at times when calcium currents were modified.

The slow reduction in hERG/I_{Kr} processing and surface expression is a direct consequence of the interference of As_2O_3 with the binding of two essential cytosolic chaperones, Hsp70 and Hsp90, to hERG (Ficker et al., 2003). As a result, processing of the ER-resident hERG protein into the mature cell-surface form of hERG is inhibited. Because As_2O_3 interacts preferentially with neighboring thiol groups, it is of interest that many Hsp90 proteins possess a strictly conserved thiol pair in the middle segment of the chaperone protein. It is conceivable that modification of these thiols by As_2O_3 renders Hsp90 nonfunctional (Matsumoto et al., 2002). Direct inhibition of Hsp90 by As_2O_3 is also consistent with the trafficking block of hERG induced by two specific inhibitors of Hsp90 function, geldanamycin and radicicol (Roe et al., 1999). Because Hsp90 is a previously unrecognized target for As_2O_3, our results may also further the understanding of its anticancer activity.

Although the trafficking block of hERG would be sufficient to explain the increased propensity of patients with APL treated with As_2O_3 for QT prolongation and TdP, it is not too surprising that As_2O_3, which not only modifies thiol groups but also increases the production of reactive oxygen species, exerts multiple effects on cardiac ion channels. Most prominent is the large increase in cardiac calcium currents. The modification of calcium currents by As_2O_3 is different from the acquired processing defect of hERG in that the underlying process is faster, possibly the result of a direct enzymatic modification of the calcium channel itself or of an essential accessory protein (e.g., in phosphorylation/dephosphorylation reactions).

As demonstrated with low doses of nisoldipine, the increase in calcium currents has important therapeutic implications because it suggests that calcium-channel blockers may be well-suited to normalize QT prolongation during As_2O_3 therapy. The sodium channel blocker mexiletine has already been used as part of a prophylactic therapy to reduce cardiac complications in patients with APL (Ohnishi et al., 2000). However, the use of sodium-channel blockers in the treatment of arrhythmias is controversial because of their recognized proarrhythmic properties (Balser, 2001). We provide the first experimental evidence that calcium-channel blockers may be more efficacious. In addition, previous proposals to control electrolyte imbalances in patients with APL have now gained special importance because it is well known that hERG currents are strongly modulated by extracellular potassium concentrations (Sanguinetti et al., 1995; Ohnishi et al., 2000). Taken together, the concerted action of the proarrhythmic drug As_2O_3 on two cardiac ion channel systems represents a new paradigm for acquired long QT syndrome, which may help us to understand why QT prolongation and TdP seem to be so prevalent among patients treated for acute promycelocytic leukemia.

References

Balser JR (2001) The cardiac sodium channel: gating function and molecular pharmacology. *J Mol Cell Cardiol* **33:**599–613.

Barbey JT, Pezzullo JC, and Soignet SL (2003) Effect of arsenic trioxide on QT interval in patients with advanced malignancies. *J Clin Oncol* **21:**3609–3615.

Berube J, Caouette D, and Daleau P (2001) Hydrogen peroxide modifies the kinetics of HERG channel expressed in a mammalian cell line. *J Pharmacol Exp Ther* **297:**96–102.

Chiang CE, Luk HN, Wang TM, and Ding PYA (2002) Prolongation of cardiac repolarization by arsenic trioxide. *Blood* **100:**2249–2252.

Drolet B, Simard C, and Roden DM (2004) Unusual effects of a QT-prolonging drug, arsenic trioxide, on cardiac potassium currents. *Circulation* **109:**26–29.

Ficker E, Dennis AT, Wang L, and Brown AM (2003) Role of the cytosolic chaperones Hsp70 and Hsp90 in maturation of the cardiac potassium channel HERG. *Circ Res* **92:**E87–E100.

Keating MT and Sanguinetti MC (2001) Molecular and cellular mechanisms of cardiac arrhythmias. *Cell* **104:**569–580.

Little RE, Kay GN, Cavender JB, Epstein AE, and Plumb VJ (1990) Torsade de pointes and T-U wave alternans associated with arsenic poisoning. *Pacing Clin Electrophysiol* **13:**164–170.

Liu SX, Athar M, Lippai I, Waldren C, and Hei TK (2001) Induction of oxyradicals by arsenic: implication for mechanism of genotoxicity. *Proc Natl Acad Sci USA* **98:**1643–1648.

Margeta-Mitrovic M, Jan YN, and Jan LY (2000) A trafficking checkpoint controls $GABA_B$ receptor heterodimerization. *Neuron* **27:**97–106.

Matsumoto S, Tanaka E, Nemoto TK, Ono T, Takagi Y, Imai J, Kimura Y, Yahara I, Kobayakawa T, Aysue T, et al. (2002) Interaction between the N-terminal and middle regions is essential for the *in vivo* function of Hsp90 molecular chaperone. *J Biol Chem* **277:**34959–34966.

Miller WH, Schipper HM, Lee JS, Singer J, and Waxman S (2002) Mechanism of action of arsenic trioxide. *Cancer Res* **62:**3893–3903.

Myers MA (1998) Direct measurement of cell numbers in microtitre plate cultures using the fluorescent dye SYBR green I. *J Immunol Methods* **212:**99–103.

Nerbonne JM (2000) Molecular basis of functional voltage-gated K^+ channel diversity in the mammalian myocardium. *J Physiol* **525:**285–298.

Ohnishi K, Yoshida H, Shigeno K, Nakamura S, Fujisawa S, Naito K, Shinjo K, Fujita Y, Matsui H, Takeshita A, et al. (2000) Prolongation of the QT interval and ventricular tachycardia in patients treated with arsenic trioxide for acute promyelocytic leukemia. *Ann Intern Med* **133:**881–885.

Redfern WS, Carlsson L, Davis AS, Lynch WG, MacKenzie I, Palethorpe S, Siegl PKS, Strang I, Sullivan AT, Wallis R, et al. (2003) Relationships between preclinical cardiac electrophysiology, clinical QT interval prolongation and torsade de pointes for a broad range of drugs: evidence for a provisional safety margin in drug development. *Cardiovasc Res* **58:**32–45.

Roe SM, Prodromou C, O'Brien R, Ladbury JE, Piper PW, and Pearl LH (1999) Structural basis for the inhibition of the hsp90 molecular chaperone by the antitumor antibiotics radicicol and geldanamycin. *J Med Chem* **42:**260–266.

Sanguinetti MC, Jiang C, Curran ME, and Keating MT (1995) A mechanistic link between an inherited and an acquired cardiac arrhythmia: HERG encodes the I_{Kr} potassium channel. *Cell* **81:**299–307.

Shen ZX, Chen GQ, Ni JH, Li XS, Xiong SM, Qiu QY, Zhu J, Tang W, Sun GL, Yang KQ, et al. (1997) Use of arsenic trioxide (As_2O_3) in the treatment of acute promyelocytic leukemia (APL): II. Clinical efficacy and pharmacokinetics in relapsed patients. *Blood* **89:**3354–3360.

Soignet SL, Frankel SR, Douer D, Tallman MS, Kantarjian H, Calleja E, Stone RM, Kalaycio M, Scheinberg DA, Steinherz P, et al. (2001) United States multicenter study of arsenic trioxide in relapsed acute promyelocytic leukemia. *J Clin Oncol* **19:**3852–3860.

St. Petery J, Gross C, and Victoria BE (1970) Ventricular fibrillation caused by arsenic poisoning. *Am J Dis Child* **120:**367–371.

Taglialatela M, Castaldo P, Iossa S, Pannaccione A, Fresi A, Ficker E, and Annunziato L (1997) Regulation of the human ether-a-gogo related gene (HERG) K^+ channels by reactive oxygen species. *Proc Natl Acad Sci USA* **94:**11698–11703.

Unnikrishnan D, Dutcher JP, Varshneya N, Lucarielle R, Api M, Garl S, Wiernik PH, and Chiaramida S (2001) Torsade de pointes in 3 patients with leukemia treated with arsenic trioxide. *Blood* **97:**1514–1516.

Westervelt P, Brown RA, Adkins DR, Khoury H, Curtin P, Hurd D, Luger SM, Ma MK, Ley TJ, and DiPersio JF (2001) Sudden death among patients with acute promyelocytic leukemia treated with arsenic trioxide. *Blood* **98:**266–271.

Wu MH, Lin CJ, Chen CL, Su MJ, Sun SSM, and Cheng AL (2003) Direct cardiac effects of As_2O_3 in rabbits: evidence of reversible chronic toxicity and tissue accumulation of arsenicals after parenteral administration. *Toxicol Appl Pharmacol* **189:**214–220.

Zhang TD, Chen GQ, Wang ZG, Wang ZY, Chen SJ, and Chen Z (2001) Arsenic trioxide, a therapeutic agent for APL. *Oncogene* **20:**7147–7153.

Zhou Z, Gong Q, Epstein ML, and January CT (1998) HERG channel dysfunction in human long QT syndrome. *J Biol Chem* **273:**21061–21066.

Zhu J, Chen Z, Lallemand-Breitenbach V, and de The H (2002) How acute promyelocytic leukemia revived arsenic. *Nat Rev Cancer* **2:**1–9.

Address correspondence to: Dr. Eckhard Ficker, Rammelkamp Center, MetroHealth Medical Center, 2500 MetroHealth Drive, Cleveland, OH 44109. E-mail: eficker@metrohealth.org